

# Quantum dynamics simulation

PUJOL Martin

5 Mars 2023

## Table des matières

<b>1</b>	<b>Introduction</b>	<b>2</b>
<b>2</b>	<b>Materials and Methods</b>	<b>2</b>
2.1	Resolution Methods : Finding the eigen states of the Hamiltonian . . . . .	2
2.2	Resolution Methods : Simulating the dynamics of quantum states . . . . .	3
2.3	4th-Order Runge-Kutta Method . . . . .	4
2.4	Python Tools . . . . .	5
<b>3</b>	<b>Experience and Results</b>	<b>5</b>
3.1	Finding the eigen states of the Hamiltonian . . . . .	5
3.2	Simulating the dynamics of quantum states . . . . .	7
<b>4</b>	<b>Discussion of Results</b>	<b>8</b>
<b>5</b>	<b>Conclusion</b>	<b>9</b>

# 1 Introduction

The ability to describe the time evolution of a quantum system, that is, the evolution over time of its wave function  $\Psi(\vec{r}, t)$ , is one of the major results of quantum physics. Quantum mechanics is a fundamental theory of physics that has undergone considerable development in the 20th century, with numerous applications in physics, chemistry, biology, and computer science. Schrödinger's equations describe the evolution of quantum systems, and their numerical resolution is a significant challenge in theoretical physics and numerical simulation.

The numerical resolution of the time-dependent Schrödinger equations is challenging and requires adapted numerical methods, whether for one-dimensional or multidimensional systems. These methods rely on intensive computation algorithms, which demand substantial computational resources. Computational power, therefore, is a critical resource central to this study.

In this project, we implement numerical methods to solve the time-dependent Schrödinger equation for a particle of mass  $m$  subject to the action of a one-dimensional potential  $V(x)$ . This equation describes the time evolution of the particle's wave function  $\Psi(x, t)$ , given by Equation (3). The one-dimensional potential can be used to model various systems, such as particles in a potential well, electrons in a crystal, atoms in a gas, or molecules in an environment.

First, we study the stationary states of the system, corresponding to time-independent solutions of the Schrödinger equation. These stationary states are crucial in quantum physics as they determine the system's fundamental properties, such as energy levels and associated wave functions. To this end, we use the finite difference method to discretize space, replacing partial derivatives with finite differences. We also employ numerical integration methods to compute eigenvalues and eigenvectors of the matrix representing the system's Hamiltonian.

Next, we study the system's time evolution using numerical integration methods, such as Euler's method and the fourth-order Runge-Kutta method (RK4). These methods calculate the wave function  $\Psi(x, t)$  at different times  $t$ , using the initial wave function at  $t = 0$  as a starting condition. We also analyze the convergence and stability of these integration methods using numerical analysis techniques.

Finally, we compare numerical results with analytical results for simple systems, allowing us to conclude the importance of spatial and temporal discretization.

## 2 Materials and Methods

### 2.1 Resolution Methods : Finding the eigen states of the Hamiltonian

First, we aim to determine the eigenstates of the Hamiltonian. Let us recall its expression :

$$-\frac{\hbar^2}{2m} \frac{d^2\psi}{dx^2} + V(x)\psi = E\psi$$

where  $\hbar$  is the reduced Planck constant,  $m$  is the particle mass,  $V(x)$  is the potential, and  $E$  is the eigenvalue associated with the stationary state  $\psi$ .

We seek to solve this equation to find the eigenvalues of the Hamiltonian. To do so, we discretize the spatial domain using a finite difference method. By discretizing the space, the second derivative is replaced with a centered finite difference, leading to the following equation :

$$-\frac{\hbar^2}{2m} \frac{\psi_{i+1} - 2\psi_i + \psi_{i-1}}{\Delta x^2} + V_i\psi_i = E\psi_i$$

where  $i$  is the discrete index representing the spatial position along the  $x$  direction, and  $\Delta x$  is the distance between discrete points. This equation can be rewritten in matrix form as :

$$\mathbf{H}\psi = E\psi$$

where  $\mathbf{H}$  is the Hamiltonian matrix,  $\psi$  is the discretized wavefunction vector, and  $E$  is the discretized eigenvalue.

Using the finite difference method, the matrix  $\mathbf{H}$  becomes tridiagonal with specific diagonal and off-diagonal elements. The main diagonal is given by :

$$\mathbf{H}_{ii} = \frac{\hbar^2}{m\Delta x^2} + V_i$$

and the off-diagonal terms are :

$$\mathbf{H}_{i,i+1} = \mathbf{H}_{i+1,i} = -\frac{\hbar^2}{2m\Delta x^2}$$

Next, to find the eigenvalues of the Hamiltonian matrix, we apply a tridiagonal diagonalization method.

This method allows us to diagonalize the Hamiltonian matrix to obtain discrete eigenvalues and their corresponding eigenvectors. These eigenvalues and eigenvectors represent the discrete energy levels and wavefunctions, respectively.

In summary, the finite difference method enables us to discretize the stationary wave equation and find the eigenfunctions of the Hamiltonian in a discrete framework.

## 2.2 Resolution Methods : Simulating the dynamics of quantum states

In the second part, we studied the time evolution of the wavefunction of a particle in a one-dimensional potential by solving the time-dependent Schrödinger equation :

$$i\hbar \frac{\partial}{\partial t} \Psi(x, t) = \hat{H} \Psi(x, t)$$

where  $\hbar$  is the reduced Planck constant, and  $\hat{H}$  is the Hamiltonian operator of the system. To derive a differential relationship for the wavefunction  $\Psi(x, t)$ , we used the Hamiltonian operator for a particle in a one-dimensional potential :

$$\hat{H} = -\frac{\hbar^2}{2m} \frac{\partial^2}{\partial x^2} + V(x)$$

where  $m$  is the particle mass, and  $V(x)$  is the one-dimensional potential.

By substituting the Hamiltonian operator into the Schrödinger equation, we obtain :

$$i\hbar \frac{\partial}{\partial t} \Psi(x, t) = -\frac{\hbar^2}{2m} \frac{\partial^2}{\partial x^2} \Psi(x, t) + V(x) \Psi(x, t)$$

We then discretized the spatial domain, replacing the continuous wavefunction with discrete values  $\Psi_j^n$ , where  $j$  represents the spatial position, and  $n$  represents the time step. Partial derivatives are replaced with finite differences to derive a recurrence relation for the discrete wavefunction values :

$$i\hbar \frac{\Psi_j^{n+1} - \Psi_j^n}{\Delta t} = -\frac{\hbar^2}{2m} \frac{\Psi_{j+1}^n - 2\Psi_j^n + \Psi_{j-1}^n}{\Delta x^2} + V_j \Psi_j^n$$

where  $\Delta x$  and  $\Delta t$  are the spatial and temporal discretization steps, respectively, and  $V_j$  is the potential value at position  $j\Delta x$ . This recurrence relation is known as the explicit Euler method for solving the time-dependent Schrödinger equation.

Additionally, we used more precise numerical integration methods, such as the 4th-order Runge-Kutta method (RK4). In this case, a more complex recurrence relation is used.

## 2.3 4th-Order Runge-Kutta Method

Next, we will use another method : the 4th-order Runge-Kutta method. For this algorithm, we have :

$$\Psi(x, t + 1) = \Psi(x, t) + dt \cdot \left( \frac{1}{6}k_1 + \frac{1}{3}k_2 + \frac{1}{3}k_3 + \frac{1}{6}k_4 \right) \quad (1)$$

with :

$$\begin{aligned} k_1 &= f(\Psi(x, t)) \\ k_2 &= f\left(\Psi\left(x + \frac{1}{2}dt \cdot k_1, t + \frac{dt}{2}\right)\right) \\ k_3 &= f\left(\Psi\left(x + \frac{1}{2}dt \cdot k_2, t + \frac{dt}{2}\right)\right) \\ k_4 &= f(\Psi(x + dt \cdot k_3, t + dt)) \end{aligned}$$

Here, since  $H$  is time-independent, we can have :

$$\begin{aligned} k_1 &= f(\Psi(x, t)) \\ k_2 &= f\left(\Psi\left(x + \frac{1}{2}dt \cdot k_1, t\right)\right) \\ k_3 &= f\left(\Psi\left(x + \frac{1}{2}dt \cdot k_2, t\right)\right) \\ k_4 &= f(\Psi(x + dt \cdot k_3, t)) \end{aligned}$$

We will note that this algorithm is much more efficient than the Euler method. Indeed, for the same  $dt$ , even if it is small, this method allows us to obtain a consistent result. This is due to the fact that the 4th-order Runge-Kutta method is an additional step in refining the integral calculation. Instead of using the left rectangle method like Euler, we use the trapezoidal method for 2nd-order Runge-Kutta and Simpson's method for 4th-order Runge-Kutta

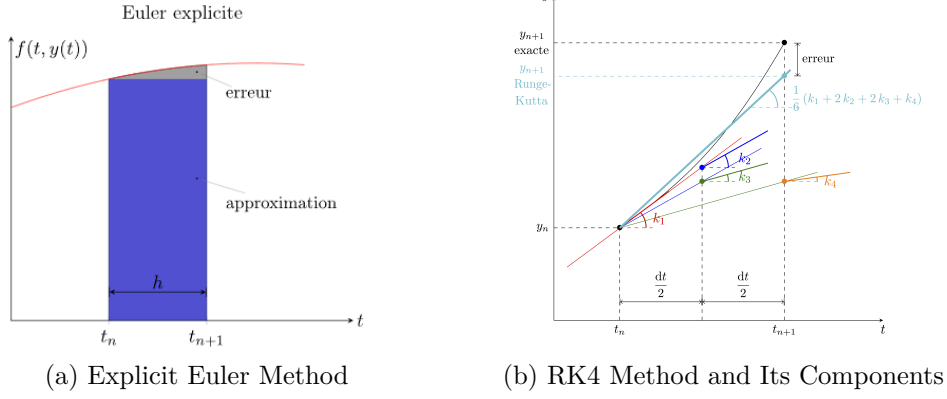


FIGURE 1 – Differences between the Euler and 4th-order Runge-Kutta methods

## 2.4 Python Tools

In this project, various Python libraries were utilized to simulate the dynamics of a Gaussian wave packet in different potentials. First, the NumPy library was employed to manipulate multidimensional arrays, enabling efficient vectorized calculations and optimizing performance.

Next, the Matplotlib library was used for plotting graphs and creating animations. Matplotlib.pyplot was leveraged to plot graphs of the temporal evolution of the wavefunction and the associated particle's mean position. Additionally, Matplotlib.animation was used to create corresponding animations.

The Numba library was also utilized to optimize the performance of calculations.

## 3 Experience and Results

### 3.1 Finding the eigen states of the Hamiltonian

In summary, these Python libraries allowed for effective and precise simulation of wavefunction dynamics in various potentials, combining code optimization, graphical visualization, and numerical resolution of differential equations.

If we consider a particle in an infinite square well of width  $L$ , the wave functions that are solutions to the time-independent Schrödinger equation are zero outside the well and have the following form inside the well :

$$\psi_p(x) = \sqrt{\frac{2}{L}} \sin\left(\frac{(p+1)\pi(x + \frac{L}{2})}{L}\right)$$

The energies of these states are given by :

$$E_p = \frac{\hbar^2}{2m} \left(\frac{\pi(p+1)}{L}\right)^2$$

Note : Here, we choose  $\frac{\hbar^2}{2m} = 1$ .

The second case where the solution is known is the harmonic potential :

$$V(x) = \frac{1}{2}kx^2 = \frac{1}{2}m\omega^2x^2, \quad \omega = \sqrt{\frac{k}{m}}$$

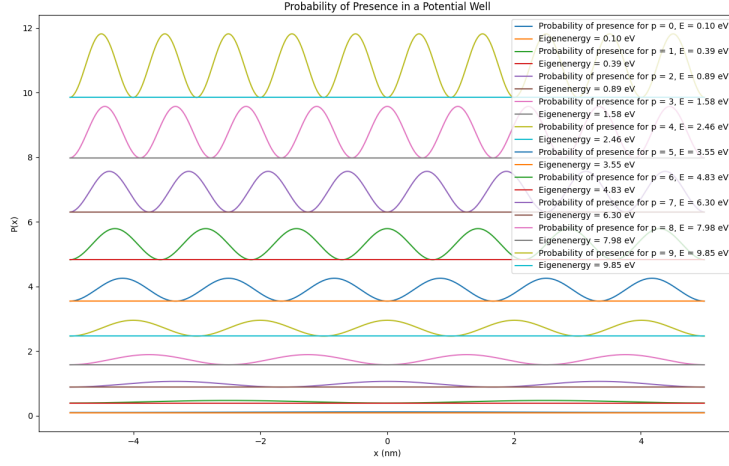


FIGURE 2 – infinite-well-potential

The eigenenergies are now written as :

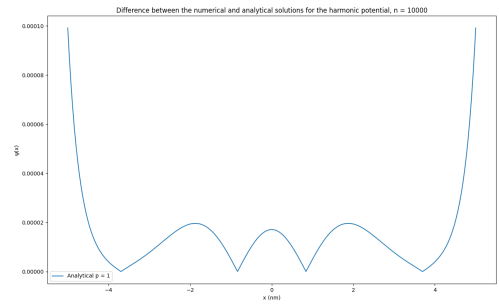
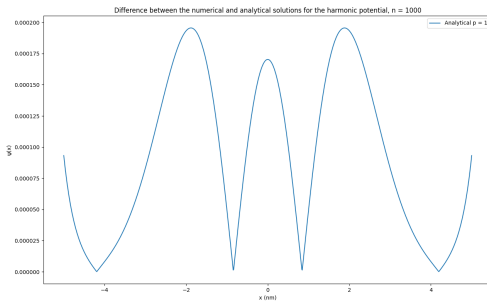
$$E_p = \left(p + \frac{1}{2}\right) \hbar\omega, \quad p = 0, 1, 2, 3, \dots$$

The ground state, for  $p = 0$ , thus has an energy  $E_0 = \frac{\hbar\omega}{2}$ . The wave functions become :

$$\psi_p(x) = \frac{1}{\sqrt{\sigma_0 \sqrt{\pi} 2^p p!}} H_p\left(\frac{x}{\sigma_0}\right) e^{-\frac{x^2}{2\sigma_0^2}}$$

where  $\sigma_0 = \sqrt{\frac{\hbar}{m\omega}}$  and  $H_p$  is a Hermite polynomial.

We also look at a specific harmonic from the latest to look at the error of the finite element method ( $n = 100$ )

FIGURE 3 – Harmonic potential wavefunctions for  $n = 1000$  and for  $n = 10000$ 

Figures 2 to 8 illustrate the computed wavefunctions for different potentials, such as double wells, damped potential barriers, periodic potentials, and electronic potentials. The probability densities show highly satisfactory shapes, reminiscent of patterns commonly observed in physics. The results also exhibit the conservation of system symmetry properties and energy level quantization. Each graph depicts ten probability densities, offset by their respective eigenenergies.

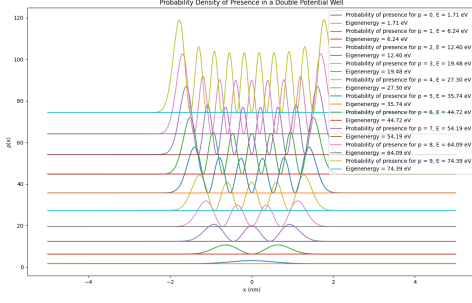


FIGURE 4 – Double-well potential

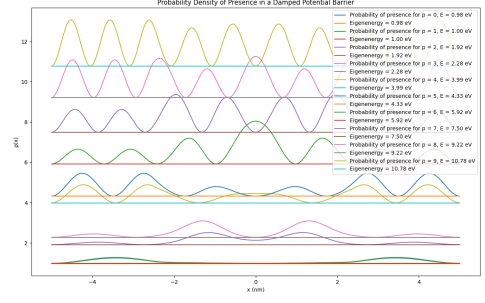


FIGURE 5 – Damped potential barrier

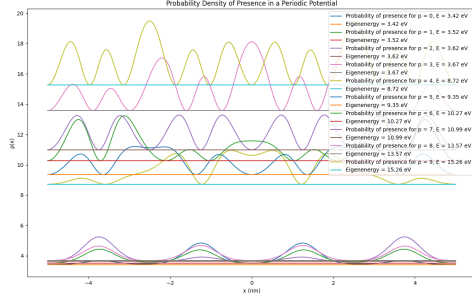


FIGURE 6 – Periodic potential

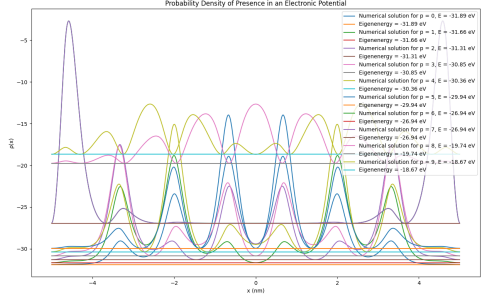


FIGURE 7 – Electronic potential

FIGURE 8 – Wavefunctions for various potentials

### 3.2 Simulating the dynamics of quantum states

First, it was necessary to determine the optimal values for  $\Delta t$  and  $\Delta x$  for simulations. To minimize spatial discretization, a minimum value of  $\Delta x = 0.1$  was chosen for a domain of length 10. This limit was essential due to the iterative nature of the calculations. Considering the differential equation, it was expected that the ratio  $\Delta t/(\Delta x)^2$  should not be too large. To confirm this hypothesis, a graph of the error over time was plotted for three different  $\Delta t$  values. The error was measured by ensuring that the probability distribution of an eigenstate does not change.

The temporal evolution of a quantum eigenstate is given by :

$$\psi(x, t) = \psi(x, 0)e^{-iEt/\hbar}$$

where  $\psi(x, 0)$  is the initial wave function,  $E$  is the energy of the eigenstate, and  $\hbar$  is the reduced Planck's constant.

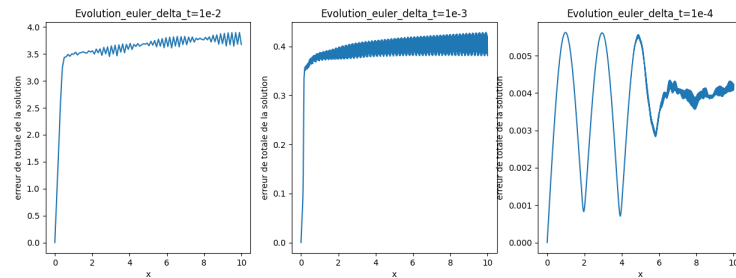


FIGURE 9 – Error evolution for the Euler method

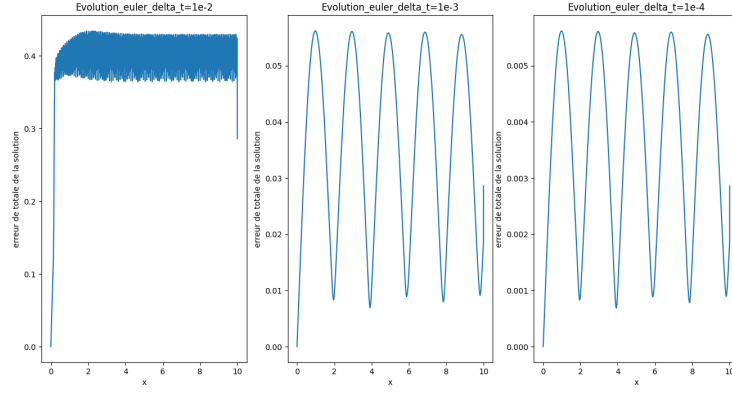


FIGURE 10 – Error evolution for the Runge-Kutta 4 method

The graphs show the error evolution for the Euler method and the Runge-Kutta 4 (RK4) method over time for different  $\Delta t$  values. It can be observed that, for a large  $\Delta t$ , the error increases rapidly, whereas for a sufficiently small  $\Delta t$ , the error remains low and stable. Overall, the RK4 method is more accurate than the Euler method for all tested  $\Delta t$  values. Therefore, simulations were continued with the RK4 method and  $\Delta t = 1e-3$ .

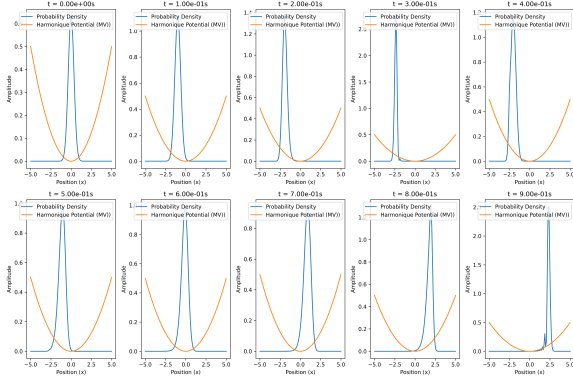


FIGURE 11 – Wave packet dynamics in a harmonic potential

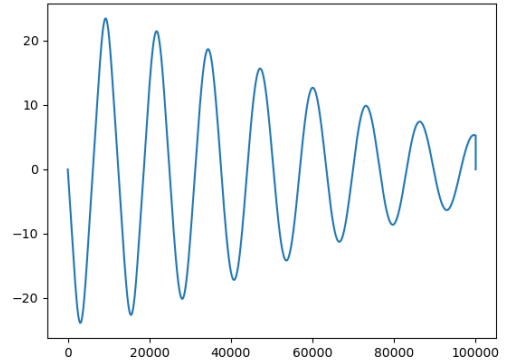


FIGURE 12 – Mean position of the particle

Figure 11 shows the oscillation of a wave packet in a harmonic potential. To achieve a significant displacement, the wave packet was assigned very high energy ( $k_0 = 1e10$ ). However, the wave packet's position spreads over time, possibly due to numerical errors. Moreover, the particle's mean position exhibits a periodic oscillation, seemingly converging toward zero. This observation reflects the quasi-classical behavior of the particle in a harmonic potential.

Figures 13 extend the previous simulations, showing a wave packet traversing a potential field composed of six uniformly spaced electrons. It can be observed that the wave packet appears trapped at the center, where the potential is highest.

## 4 Discussion of Results

The discussion can be structured into two main parts : numerical methods and observed results.

The first part of the study focused on solving the eigenstates of the Hamiltonian for various potentials. The initial objective was to determine the optimal value of  $\Delta t$  to minimize the error



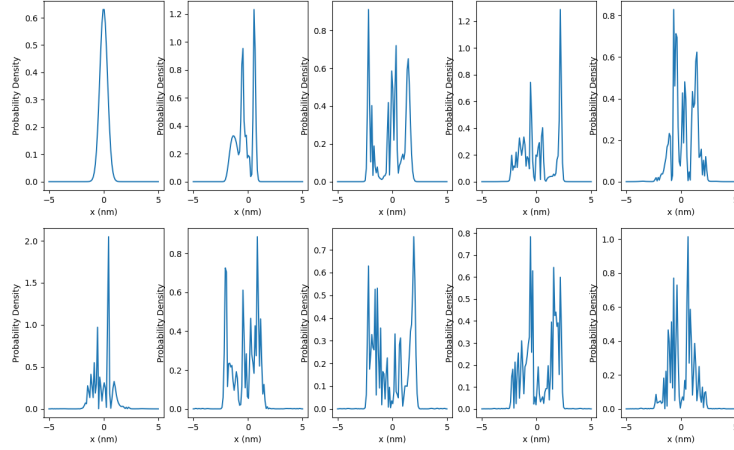


FIGURE 13 – Wave packet dynamics in an electronic potential

while limiting computation time. Graphs depicting errors for  $\Delta t = 1e-2$  and  $\Delta t = 1e-3$  showed a significant reduction in error for smaller  $\Delta t$  values but at the cost of increased computation time. Thus,  $\Delta t = 1e-3$  was chosen as a reasonable compromise.

The following graphs presented the computed eigenfunctions for various potentials. The resulting probability densities were highly satisfactory, showing patterns consistent with the expected physical properties for each potential, while preserving system symmetry and energy quantization.

In the second part, we examined the temporal evolution of wavefunctions. Optimal  $\Delta t$  and  $\Delta x$  values were determined, ensuring that  $\Delta t/(\Delta x)^2$  remained small. The error evolution graphs for different  $\Delta t$  values validated this approach.

Regarding the results, it was reassuring to find quantized energy levels and correct analytical solutions for the initial energy levels in the infinite square well and harmonic potential. The shapes of the probability densities were also consistent with expectations. A key confirmation of these calculations was the invariance of wavefunctions over time, in contrast to their linear combinations or wave packets.

Finally, the dynamics of wavefunctions revealed further insights. For example, the periodic oscillation of a Gaussian wave packet in a harmonic potential suggested quasi-classical behavior. Additionally, the trapping of a wave packet by multiple electrons highlighted the quantum mechanical phenomenon of localization.

## 5 Conclusion

This project successfully implemented numerical methods to solve the time-dependent Schrödinger equation based on the system Hamiltonian. The results demonstrated the importance of carefully selecting  $\Delta t$  and  $\Delta x$  to balance accuracy and computational feasibility. The study highlighted the precision of the RK4 method over the Euler method, albeit at a higher computational cost.

The investigation revealed quantized energy levels, consistent analytical predictions, and preserved system symmetry. Additionally, the dynamics of Gaussian wave packets in harmonic and electronic potentials provided valuable insights into quasi-classical behavior and quantum localization.

In summary, the project tackled the understanding and application of numerical methods for solving the time-dependent Schrödinger equation, showcasing the quantum properties and

dynamics of different systems.